Dalton Transactions

PAPER

View Article Online
View Journal | View Issue

Cite this: *Dalton Trans.*, 2014, **43**, 11502

Cryogenic magneto-caloric effect and magneto-structural correlations in carboxylate-bridged Gd(III) compounds†

O. Roubeau,*[a] G. Lorusso,[a] S. J. Teat[b] and M. Evangelisti[a]

Received 7th March 2014,
Accepted 17th April 2014

DOI: 10.1039/c4dt00697f

www.rsc.org/dalton

Two new infinite coordination chain compounds $[Gd(CH_3CO_2)_3(dmf)]_\infty$ (**1**) and $\{[Gd(HO(CH_2)_3CO_2)_3(H_2O)]\cdot H_2O\}_\infty$ (**2**) have been obtained attempting to modify a prototype molecular cooler. The structures of both compounds as determined by single-crystal X-ray diffraction are reported, together with a detailed study of their magnetic and thermal properties, describing for both compounds a large magneto-caloric effect. The dominant ferromagnetic interaction present in **2** clearly favours this material at low applied magnetic fields, with respect to **1** that exhibits antiferromagnetic interactions. Magneto-structural correlations of the sign and strength of the magnetic interactions are derived for carboxylato-bridged Gd(III) systems.

Introduction

Certain molecular or molecular-based compounds are recognized as good candidates for magnetic refrigeration at liquid helium temperature.[1] This is because of the large magneto-caloric effect (MCE) exhibited by these materials at temperatures typically below 10 K, *i.e.* a large variation of magnetic entropy (ΔS_m) and adiabatic temperature (ΔT_{ad}) induced by a magnetic field change.[1,2] As for conventional cryogenic magnetic refrigerants, *e.g.*, Gadolinium Gallium Garnet (GGG),[3] these so-called molecular coolers usually contain gadolinium because the isotropic Gd(III) ion has zero orbital angular momentum and provides the largest entropy per single ion. Although both homo- and heterometallic high nuclearity complexes have been reported to have high MCE,[4–6] small light-weight Gd(III) compounds represent the best compromise in terms of weak magnetic interactions, magnetic/non-magnetic element ratio and spin multiplicity.[2b,7,8] Enhancement of the latter through intramolecular ferromagnetic exchange is of course welcome, as it helps reaching large magnetic entropy values at comparatively lower applied magnetic fields. A good example of these considerations is provided by gadolinium acetate tetrahydrate, $[Gd_2(CH_3CO_2)_6(H_2O)_4]\cdot 4H_2O$ (Gd-ac in the following), whose exceptional MCE remains among the most appealing reported thus far for a truly molecular material.[1c,7]

Because the important parameter for application is the volumetric ΔS_m, Gd(III) metal–organic frameworks of various dimensionalities obtained with light and short bridging ligands have more recently provided significant improvements of MCE capacities.[9] Indeed, as long as magnetic ordering is avoided down to the target working temperature, the dimensionality of the refrigerant material has no effect,[10] while potentially giving access to high intrinsic density in the cases of continuous frameworks with small linkers and thus efficient space filling. With its sub-Kelvin ordering temperature and huge MCE, gadolinium formate actually compares favourably in terms of the Relative Cooling Power (RCP^2) with the commercially exploited GGG.[11]

After these recent achievements, we aim here at tackling two different though important aspects, *i.e.* on one hand avoiding long-range magnetic order and on the other hand providing the molecular coolers with a terminal ligand useful for covalent attachment with surfaces. We focus on the prototype Gd-ac system that exhibits antiferromagnetic order at a temperature of *ca.* 0.2 K, originating from efficient packing and a hydrogen bonding network involving lattice and co-ordinated water molecules.[7] Its MCE properties have been shown to be maintained once deposited on Si, although only through non-covalent interactions.[12] We have now replaced the coordinated water molecules and acetate ligands of Gd-ac, respectively, by dimethylformamide and hydroxybutanoate, resulting in both cases in the formation of infinite coordination chains, *i.e.* compounds $[Gd(CH_3CO_2)_3(dmf)]_\infty$ (**1**) and $\{[Gd(HO(CH_2)_3CO_2)_3(H_2O)]\cdot H_2O\}_\infty$ (**2**). Their single-crystal

[a]*Instituto de Ciencia de Materiales de Aragón (ICMA), CSIC and Universidad de Zaragoza, Plaza San Francisco s/n, 50009 Zaragoza, Spain.*
E-mail: roubeau@unizar.es; Fax: +34 976 761229; Tel: +34 976 762461
[b]*Advanced Light Source, Berkeley Laboratory, 1 Cyclotron Road, Berkeley, CA 94720, USA*

†Electronic supplementary information (ESI) available: Additional figures showing labelled views of the structures of **1** and **2**, magnetic and thermal properties of **1** and **2**, details of magneto-structural correlation data and additional correlations. CCDC 971619–971620. For ESI and crystallographic data in CIF or other electronic format see DOI: 10.1039/c4dt00697f

X-ray structures, magnetic and thermal properties are reported, showing respectively weak antiferro- and ferromagnetic interactions, and a large MCE in both cases. The opposite sign of the exchange interaction is discussed in light of magnetostructural considerations, and the resulting effect on the respective MCE is highlighted, especially at low applied fields.

Experimental

Synthesis

Commercial Gd_2O_3 (99.9% trace metal basis, Aldrich), 4-hydroxybutanoic acid lactone (or γ-butyrolactone, 98% Aldrich) and analytical grade glacial acetic acid, *N*,*N*′-dimethylformamide (dmf), absolute ethanol and diethylether were used without further purification, under aerobic conditions.

$[Gd(CH_3CO_2)_3(dmf)]_\infty$ (1). Crystals of $[Gd_2(CH_3CO_2)_6(H_2O)_4]\cdot 4H_2O$ (100 mg, 0.12 mmol), prepared from Gd_2O_3 and acetic acid as described previously,[7] were dissolved in dmf (20 mL), and the solution covered. Standing at room temperature of the colourless solution resulted after *ca.* 48 hours in the formation of colourless block/cube crystals of **1**, suitable for X-ray crystallography. Crystals were recovered by filtration, washed with little dmf and dried *in vacuo*. The yield was 70% (69 mg) based on Gd. Elemental analyses (wt%); calcd for $C_9H_{16}GdNO_7$ (found for **1**): C 26.53 (26.4), H 3.96 (4.0), N 3.44 (3.5). Main IR bands (neat): 1650, 1535, 1451, 1409, 1050, 1022, 963, 942, 680, 607 cm^{-1}.

$\{[Gd(HO(CH_2)_3CO_2)_3(H_2O)]\cdot H_2O\}_\infty$ (2). Gd_2O_3 (0.50 g, 1.37 mmol) was added to a white suspension of excess 4-hydroxybutanoic acid lactone (3.51 g, 40.8 mmol) in hot water (20 mL), and the resulting suspension was stirred at 90 °C for 15 min. Aqueous NaOH (1 M, 1 mL) was then added resulting in a colourless solution after 1 hour at 90 °C. The solution was filtered hot, and the filtrate was left to slowly evaporate. Colourless crystals of **2** suitable for X-ray crystallography were formed when the remaining volume was <1 mL. Bulk white polycrystalline **2** is obtained upon further evaporation to almost dryness. The bulk solid was recovered and filtered with an EtOH–diethylether 1 : 4 mixture, washed with little cold water and dried *in vacuo*. The total yield was 50% (690 mg) based on Gd. Elemental analyses (wt%); calcd for $C_{12}H_{25}GdO_{11}$ (found for **2**): C 28.68 (28.6), H 5.01 (4.9). Main IR bands (neat): 3490, 3235, 2934, 2872, 1767, 1671, 1562, 1524, 1429, 1408, 1355, 1287, 1272, 1226, 1163, 1057, 1036, 991, 965, 919, 890, 751, 721, 627, 579, 491 cm^{-1}.

Physical measurements

Infra-red spectra of neat samples were recorded on Perkin-Elmer Spectrum 100 apparatus equipped with an ATR device. Elemental analyses were performed by the Servei de Microanalisi, Consejo Superior de Investigaciones Científicas (CSIC) of Barcelona. Magnetic measurements were performed on bulk microcrystalline powders using a commercial SQUID magnetometer of the Physical Measurements unit of the Servicio General de Apoyo a la Investigación-SAI, Universidad de Zaragoza. Correction for the experimentally measured contribution of the sample holder and the sample diamagnetism, estimated from Pascal's tables, were applied. Heat capacities in the range 0.35–30 K were obtained using the relaxation method in a commercial ^{3}He set-up equipped with a 14 T magnet, also of the SAI Physical Measurements. Apiezon-N grease was used to provide good internal thermal contact between the heater, thermometer and sample, in the form a pellet made out of bulk microcrystalline powder.

Table 1 Crystal data and structure refinement for compounds **1** and **2**

	1	**2**
T [K]	100	100
Empirical formula	$C_9H_{16}GdNO_7$	$C_{12}H_{25}GdO_{11}$
FW	407.48	502.57
Wavelength [Å]	0.7107	0.7749
Crystal system	Monoclinic	Monoclinic
Space group	$P2_1/c$	$P2_1/n$
a [Å]	9.4084(5)	6.2169(4)
b [Å]	17.0945(9)	10.5404(6)
c [Å]	8.1850(4)	25.9134(15)
β [°]	93.862(2)	92.920(1)
V [Å^3]	1313.42(12)	1695.86(18)
Z	4	4
ρ [g cm^{-3}]	2.061	1.868
Reflections	3388	4728
Parameters	168	226
Restraints	0	8
R_{int}	0.0252	0.0484
R_1 [$I > 2\sigma(I)$][a]	0.0167	0.0331
wR_2 [$I > 2\sigma(I)$][b]	0.0397	0.0720
R_1 [all data][a]	0.0178	0.0449
wR_2 [all data][b]	0.0405	0.0761
Goodness-of-fit	1.091	1.055

[a] $R_1 = \sum||F_o| - |F_c||/\sum|F_o|$. [b] $wR_2 = \{\sum[w(F_o^2 - F_c^2)^2]/\sum[w(F_o^2)^2]\}^{1/2}$.

X-ray crystallography

Data for compound **1** were obtained at 100 K on a colourless block using Mo K_α radiation (λ = 0.7107 Å) on a Bruker APEX II QUAZAR diffractometer equipped with a microfocus multilayer monochromator. Data for compound **2** were collected on a colourless plate at 100 K with a Bruker APEX II CCD diffractometer on the Advanced Light Source beamline 11.3.1 at Lawrence Berkeley National Laboratory, from a silicon 111 monochromator (λ = 0.7749 Å). All data reduction and absorption corrections were performed with SAINT and SADABS.[13] Both structures were solved by direct methods and refined on F^2 using the SHELX-TL suite.[14] Crystallographic and refinement parameters are summarized in Table 1. All details can be found in the supplementary crystallographic data for this paper in cif format with CCDC numbers 971619 and 971620.

Results and discussion

Synthesis and crystal structures

Among truly molecular coolers, $[Gd_2(CH_3CO_2)_6(H_2O)_4]\cdot 4H_2O$ or Gd_2-ac remains an optimal material, resulting from high

density and one of the largest ferromagnetic interaction within Gd(III) pairs.[7] However, the dense packing of molecules through hydrogen bonds results in a dipolar magnetic order around 0.2 K, impeding cooling to lower temperatures. In order to destroy this magnetic order or bring it to lower temperatures while maintaining the dinuclear core of Gd_2-ac, we attempted replacing the coordinated and lattice water molecules of Gd_2-ac by molecules less prone to intermolecular interactions. We thus recrystallized Gd_2-ac from dmf solution, resulting in the formation of cube-shaped colourless crystals of $[Gd(CH_3CO_2)_3(dmf)]_\infty$ (**1**). Having successfully replaced water molecules and maintained similar Gd *vs.* non-magnetic weight ratio and density, the synthetic system has however evolved into coordination chains. A similar chain compound had been previously formed by reaction of Gd_2-ac with acetylacetone in methanol, confirming the tendency to form extended structures.[15] Compound **1** crystallizes in the monoclinic $P2_1/c$ space group with an asymmetric unit comprising a Gd(III) metal ion coordinated by three acetate ions and a terminal dmf molecule. The unique Gd site is nine-coordinated with Gd–O bond distances ranging from 2.3473(14) to 2.5445(16) Å forming a capped square antiprism coordination sphere. The structure is solely built on chains running along the *c*-axis (Fig. 1 top, Fig. S1† for atom labelling), in which the neighbouring Gd(III) ions are bridged by two μO:κ^{2}OO and one μOO *syn–syn* acetate groups, with a Gd···Gd separation of 4.100 Å. The μO:κ^{2}OO acetate groups are chelating the *same* Gd(III) ion, as opposed to Gd_2-ac or similar chain with methanol as the terminal ligand[15] in which the bridges are symmetric. To the best of our knowledge, this asymmetric topology of the bridge in **1** is unprecedented in carboxylate-based Gd(III) compounds.[16] The bridge through oxygen O3 has rather unequal Gd–O distances, at 2.3833(14) and 2.5238(13) Å, while those through O1 are similar, *i.e.* 2.4467(14) and 2.4666(14) Å, and so are the Gd–O–Gd angles, at 113.12(6) and 113.30(6)° respectively (Fig. S1†). The successive bridges (*i.e.* the Gd–O1–O3–Gd planes) are tilted by 59.8°, but the chain remains quite linear with a Gd···Gd···Gd angle of 174.15°, the dmf molecules pointing towards approximately the same direction. Indeed the methyl groups of these dmf molecules make a relatively short C–H···O contact with the neighbouring chain along the *a* axis (Fig. 1, bottom). This is actually the only significant interchain interaction in the crystal packing, confirming the better isolation obtained through the dmf molecules. Shortest interchain Gd···Gd separations are 9.408, *i.e.* the *a*-axis vector, and 8.732 Å along the *b*-axis. Adjacent chains along the *b*-axis direction are rotated by 180° with respect to the chain axis *c* (Fig. 1, bottom).

Molecular coolers such as Gd-ac are candidates to provide on-chip devices with efficient local refrigeration,[12] but for this purpose a strong interaction of the molecules with the surface, ideally through covalent binding, is required. We therefore attempted to make a compound similar to Gd-ac, using a carboxylic acid with a terminal ligand allowing further reactivity. Hydroxybutanoic acid was considered a good candidate for this, in particular because its propyl arm would provide some flexibility, while still maintaining a reasonably high Gd *vs.* non-magnetic element weight ratio. The reaction of excess 4-hydroxybutanoic acid lactone, a precursor of hydroxybutanoic acid, with gadolinium oxide under aqueous basic conditions resulted in the formation of another coordination chain compound, $\{[Gd(HO(CH_2)_3CO_2)_3(H_2O)]\cdot H_2O\}_\infty$ (**2**). Considering that a similar reaction using pentanoic acid resulted in a dinuclear complex,[17] the probable factor favouring the chain propagation in **2** is the ability of the flexible hydroxypropyl arm to bend and form intrachain hydrogen bonding (see below).

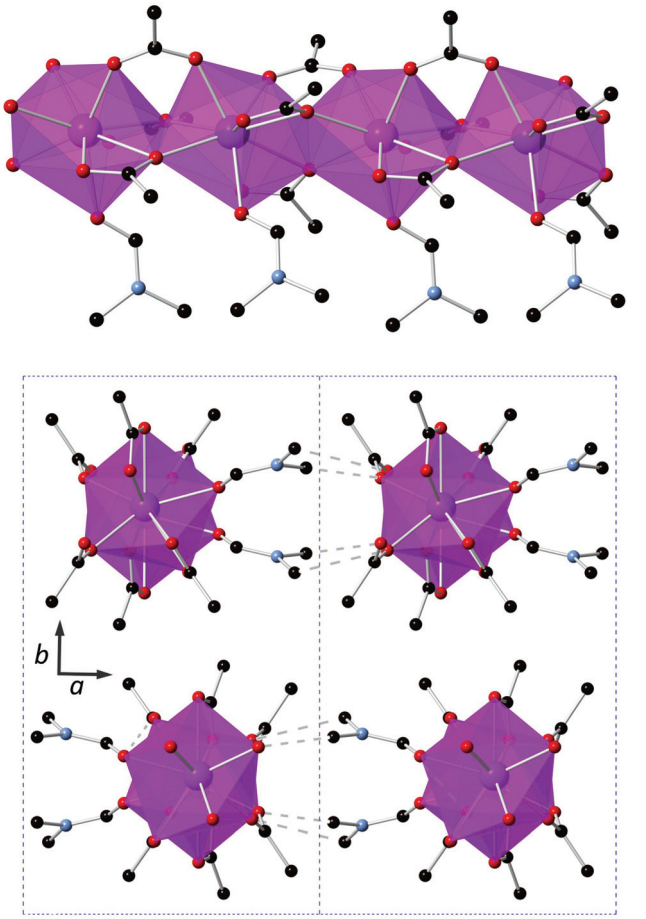

Fig. 1 Top: a view of the coordination chains in **1**, propagating along the *c*-axis. Bottom: a view of the packing along the chain axis, showing interchain C–H···O contacts as dashed grey lines and the cell limits as light blue dashed lines. Colour code: purple, Gd; red, O; light blue, N; black C. Hydrogens are omitted for clarity. Atom labeling in Fig. S1.†

Compound **2** crystallizes in the monoclinic $P2_1/n$ space group with an asymmetric unit comprising a unique Gd(III) site coordinated by two bridging and one terminal chelating hydroxybutanoate ions and an aqua ligand and a lattice water molecule. The extended chain structure along the *a*-axis (Fig. 2 top, Fig. S2† for atom labelling) builds on two very similar successive symmetric double μO:κ^{2}OO carboxylic bridges with Gd···Gd separations of 4.140 and 4.083 Å, Gd–O–Gd angles of 113.70(10) and 113.05(10) and Gd–O bond distances of

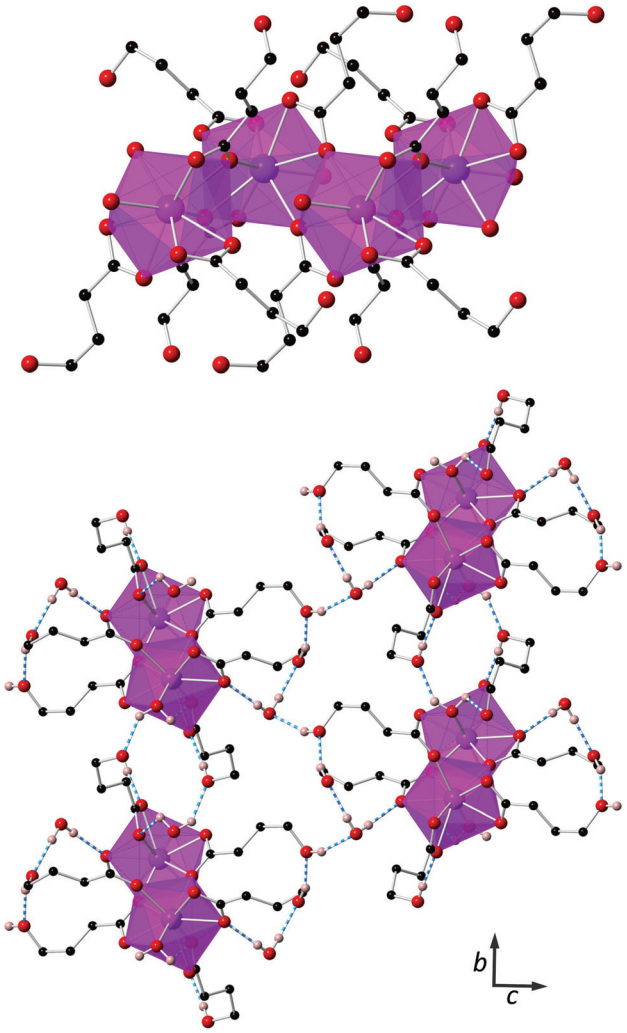

Fig. 2 Top: a view of the zig-zag coordination chains in **2**, propagating along the *a*-axis. Hydrogens are omitted for clarity. Bottom: a view of the packing along the chain axis, showing interchain hydrogen bonds as dashed blue sticks. Colour code: purple, Gd; red, O, light blue; N; black, C; beige, H. Only hydrogens involved in H-bonds are shown. Atom labeling in Fig. S2.†

2.411(3)/2.533(3) and 2.374(3)/2.520(3) Å, respectively, through atoms O5 and O7 (Fig. S2†). Interestingly, these bridge topology and characteristics are similar to those in Gd_2-ac (4.183 Å, 115.31°, 2.393/2.558 Å). The successive bridges (*i.e.* the Gd–O5–O5–Gd and Gd1–O7–O7–Gd1 planes) are tilted by 87.4°, resulting in a zig-zag chain with a Gd···Gd···Gd angle of 98.23°. The chelating third butanoate carboxylic group and terminal water molecules complete for the nine-coordinate environment of the Gd site, a distorted capped square antiprism similar to a "muffin", with Gd–O bond distances ranging from 2.357(3) to 2.533(3) Å. This third hydroxybutanoate group is bent in the chain direction and its hydroxyl oxygen O3 forms an intrachain hydrogen bond with the carboxylic oxygen O2. The other two hydroxybutanoate groups, although elongated in the *c*-axis direction, also form an intrachain hydrogen bond between their respective hydroxyl groups

Table 2 Distance and angles describing the hydrogen bonding network in the structure of $\{[Gd(HO(CH_2)_3CO_2)_3(H_2O)]\cdot H_2O\}_\infty$ (**2**). See Fig. S2 for atom labelling[a]

D–H···A	D–H (Å)	H···A (Å)	D···A (Å)	D–H–A (°)
O3–H3···O2#1	0.84	1.87	2.713(4)	174.9
O6–H6···O9#2	0.890(17)	1.880(17)	2.731(5)	159(5)
O10–H10D···O1#2	0.89	2.37	2.738(4)	104.9
O1W–H2W···O4	0.888(19)	1.98(2)	2.846(4)	164(5)
O1W–H1W···O6#1	0.904(19)	1.93(3)	2.822(5)	171(5)
O10–H10C···O3#3	0.89	1.91	2.657(4)	141.6
O9–H9···O1W#4	0.84	1.93	2.720(5)	155.3

[a] Symmetry operations: #1: $1 + x, y, z$; #2: $-1 + x, y, z$; #3: $1 - x, 1 - y, -z$; #4: $1/2 - x, -1/2 + y, 1/2 - z$.

O6 and O9. The coordinated water molecule O10 also forms an intrachain hydrogen bond with the neighbouring bridging O1 atom. The lattice water molecule O1W also participates in this dense intrachain hydrogen bonding network (Fig. 2, bottom), interacting as a donor with the hydroxyl O6 and the carboxylic O4 oxygens. The shortest interchain Gd···Gd separation is 8.498 Å, in the *b*-axis direction, arising from the only direct interchain interaction through hydrogen bonding of the coordinated water molecule O10 to the bent hydroxybutanoate of the two neighbouring chains. Chains also interact in the *c*-axis direction, although through the lattice water molecule that also forms, as an acceptor, a hydrogen bond with the hydroxyl O9 atom. Each chain is thus connected to four additional neighbours, rotated by 23.35° with respect to the chain *a*, with a longer interchain Gd···Gd separation of 13.487 Å (Fig. 2 bottom). Details of this hydrogen bonding network in the structure of **2** are given in Table 2.

Magnetic and thermal properties

The variable-temperature magnetic properties of **1** and **2** are shown in the form of χT *vs.* T plot, χ being the molar magnetic susceptibility derived from direct current (dc) magnetization collected in the 2–100 K temperature range and in an applied field of 0.01 T (Fig. 3). For both compounds, the χT value at 100 K is close to that expected for a spin-only $s = 7/2$ Gd(III) ion (7.875 cm^3 K mol^{-1}). First, χT stays roughly constant as the temperature is lowered, and at approximately 20 K a decrease/increase sets in, reaching a minimum/maximum of approximately 6.0/9.3 cm^3 K mol^{-1} at 2 K, respectively, for **1**/**2**. These behaviours point at weak magnetic interactions of opposite signs, antiferromagnetic in **1** while ferromagnetic in **2**. This is confirmed by isothermal magnetizations *vs.* field at 2 K that are slightly below and above the Brillouin function for $s = 7/2$ and $g = 2$ (Fig. S3†), respectively, for **1** and **2**. The fits of the temperature-dependences of the susceptibility to the Curie–Weiss law, $\chi = C/(T - \theta_W)$ (Fig. S4†) provide the same Curie constant $C \approx 7.88$ cm^3 K mol^{-1} for both complexes, as expected for the Gd(III) ion, and the Weiss constants $\theta_W = -0.5$ K and 0.3 K for **1** and **2**, respectively. The different signs for θ_W are a further corroboration of the type of dominant interaction involved: antiferromagnetic (**1**) and ferromagnetic (**2**).

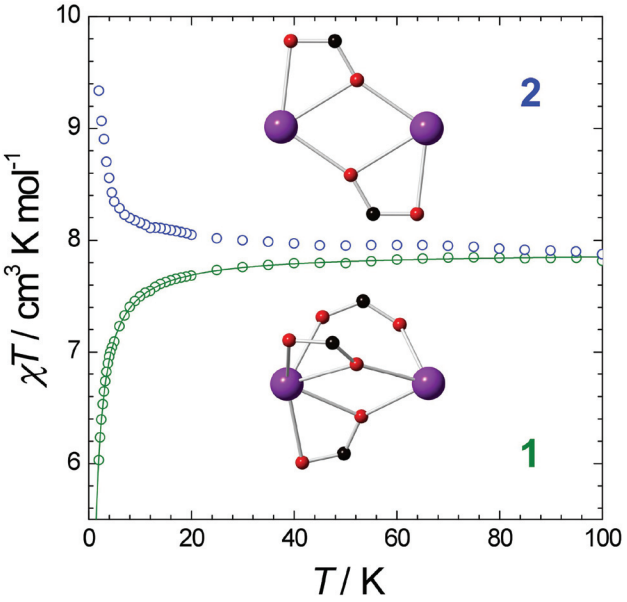

Fig. 3 Temperature-dependences (2–100 K) of the dc molar susceptibility for **1** (blue circles) and **2** (green circles) at 0.01 T applied field. The full line is the best-fit to a s = 7/2 chain model for **1**, see the main text.

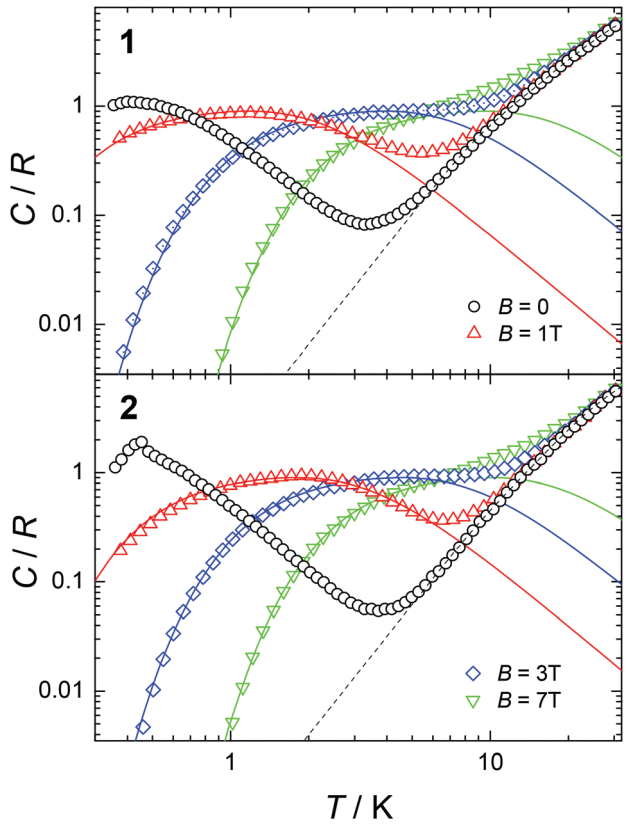

Fig. 4 Temperature-dependences (0.3–30 K) of the specific heat, normalized to Gd(III) ions and gas constant R, for **1** (top panel) and **2** (bottom panel), collected for B = 0, 1, 3 and 7 T, as labelled. The in-field data are well reproduced by Schottky calculations (solid lines) for s = 7/2 in the presence of an additional interaction field B_{int} of −0.15 T and 0.3 T respectively for **1** and **2**. Lattice contributions are reported as dashed lines.

The molar specific heat for **1** and **2** is reported in Fig. 4 for selected applied fields. The lattice contribution, C_{latt}, is modelled (dashed lines) using the Debye function, which yields the characteristic Debye temperatures θ_D = 65.6 K and 77.7 K for **1** and **2**, respectively.

For **2**, a prominent lambda-like anomaly in the zero-field specific heat occurs at T_C = 0.45 K, denoting a phase transition, whose magnetic origin is proven by the disappearance of this feature upon applying a magnetic field. The peak occurs at a temperature comparable to θ_W, suggesting that interactions propagate three-dimensionally without a preferred direction. The mean-field expression for the transition temperature, $\theta_W = z|J|s(s+1)/3k_B$, can be employed to obtain zJ/k_B = 0.052 cm^{-1}, where z is the number of nearest magnetic neighbours.

In the case of **1**, no phase transition is detected down to the lowest experimentally-accessible temperature. Thus, we tentatively associate the observed magneto-thermal properties with 1D magnetic fluctuations within the chains, depicted in Fig. 1. We model the experimental susceptibility of **1** using Fisher's expression derived for a Heisenberg chain of s = 7/2 spins and a Hamiltonian of type $-J\sum s_i s_{i+1}$.[18] The full line in Fig. 3 shows the excellent agreement that is obtained for g = 2.00 and J/k_B = −0.035 cm^{-1}. It is worth mentioning that the same model applied to **2** provides a poor description of the χ data.[19]

The specific heat measurements in applied fields, B, are characterized by Schottky-type anomalies (Fig. 4), which we analyse as follows. In a mean-field approach, the onset of exchange interactions can be interpreted in terms of an interaction field B_{int}, producing a Zeeman splitting of the (otherwise degenerate) Gd(III) spin-multiplet and, thus, leading to a Schottky-type anomaly, as observed. When measuring the specific heat in B, the total field becomes the sum of B_{int} and B, so the anomaly should shift to higher or lower temperatures, depending on the sign of B_{int}, *i.e.*, positive (for ferromagnetism) or negative (antiferromagnetism), respectively. We calculate the Schottky-type anomalies for fields $B + B_{int}$, where B_{int} is introduced as a free parameter. The best agreement with the experimental data is obtained for B_{int} = −0.15 T and 0.3 T for **1** and **2**, respectively (solid lines in Fig. 4), as expected because of the antiferromagnetic interactions in **1** and ferromagnetic interactions in **2**.

Using the specific heat data, we evaluate the magnetic entropy according to the expression $S_m(T) = \int C_m(T)/T\mathrm{d}T$, where C_m is the magnetic contribution to the specific heat, which we obtain by subtracting C_{latt} from the total heat capacity. The so-derived $S_m(T,B)$ curves for both complexes are depicted in Fig. S5.† Next, we evaluate the MCE, specifically, the magnetic entropy change $-\Delta S_m(T,\Delta B) = S_m(B_f) - S_m(B_i)$ for the magnetic field change $\Delta B = B_f - B_i$. The so-obtained results are depicted in Fig. 5, together with $\Delta S_m(T,\Delta B)$ that we derive by applying the Maxwell relation, $\Delta S_m(T,\Delta B) = \int[\partial M(T,B)/\partial T]_B \mathrm{d}B$, to the magnetization, $M(T,B)$, data (Fig. S6†). The good agreement proves the validity of both independent

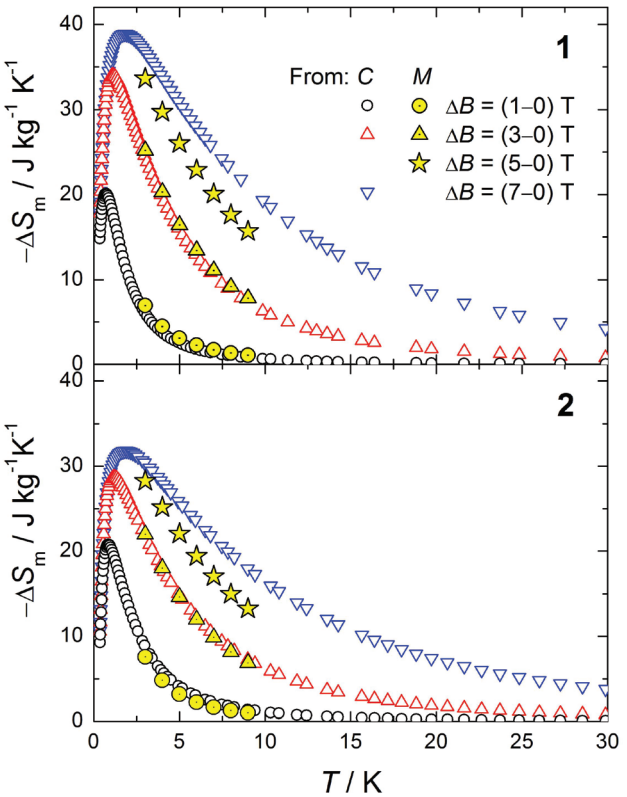

Fig. 5 Temperature-dependences of the magnetic entropy change, ΔS_m, as obtained from specific heat data, for the indicated applied-field changes ΔB, for **1** (top) and **2** (bottom). The corresponding ΔS_m values derived from magnetization data are shown as full markers for ΔB of 1, 3 and 5 T.

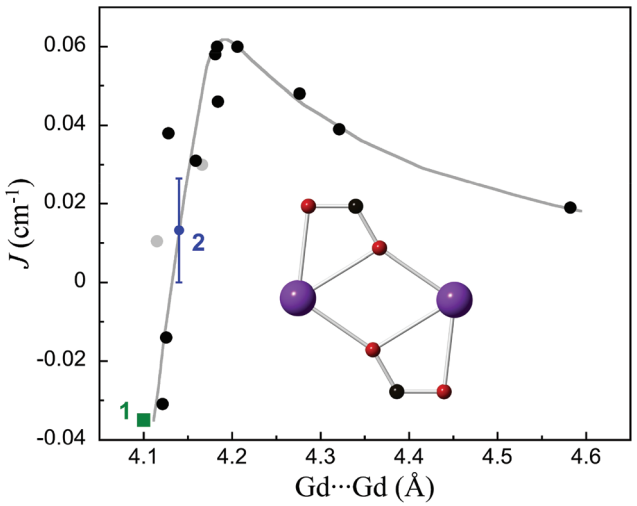

Fig. 6 Correlation of the exchange coupling in Gd(III) pairs bridged by two μO:κ²OO carboxylates (A-type, black dots) *vs.* the Gd···Gd separation. Grey dots are compounds with two different di(μO:κ²OO carboxylate) bridges for which average values of the Gd···Gd separation and the Gd–O–Gd angle have been used. The full line is a guide for the eye highlighting the reasonable correlation found. The range given for **2** derives from zJ/k_B = 0.052 cm^{-1} (see the text) and from assuming $2 < z < 6$.

approaches. For both molecules, the MCE reaches large values that are comparable to those reported in the recent literature for Gd(III)-based complexes.[1c,4,5,7,8] Fig. 5 shows that, for ΔB = 7 T, $-\Delta S_m$ reaches 38.8 J kg^{-1} K^{-1} for **1** and 31.8 J kg^{-1} K^{-1} for **2** at T = 1.8 K. It is worth mentioning that, if the entropy change is reported in mass units, then the entropy change on increasing ΔB tends to larger values in **1**, because of its relatively smaller molecular mass (by 20%). However, for the smaller field changes (*e.g.*, ΔB = 1 T), the MCE is chiefly driven by the magnetic interactions. Therefore, under these conditions, $-\Delta S_m$ is larger in **2** since antiferromagnetic interactions in **1** are detrimental to the MCE.[2b] This can be clearly evidenced by reporting the entropy changes in molar units and normalized to Gd(III), see Fig. S7.†

Magneto-structural considerations

Magnetic exchange coupling in compounds with Gd(III) ions connected through oxygen donors has been studied extensively, in particular for compounds with various types of bridge topologies based on carboxylate ligands.[7,15,17,20–23] However, no clear correlation of any specific structural parameter with the magnitude and sign of the exchange coupling has yet been found.[17,20] This is probably due in part to the weakness of the exchange couplings, which makes their accurate determination difficult, together with the variety of bridge topologies encountered. Indeed, for a variety of compounds with bridge topologies involving different bridging modes of carboxylate groups, the so-called B- and C-types *i.e.* two symmetric μO:κ²OO and respectively two or one μOO *syn–syn* carboxylates,[17,21] antiferromagnetic and ferromagnetic interactions of varying strengths have been reported.[17,20] There is though one bridge topology for which a systematic trend seems to hold. For compounds with Gd(III) pairs of the so-called A-type, *i.e.* solely bridged by two μO:κ²OO carboxylates, a ferromagnetic coupling is in most cases observed.[7,17,21,22] This trend is confirmed here with the weak ferromagnetic interaction derived in **2**. Actually, the magnitude of the interaction in these compounds does correlate with the Gd···Gd separation, although not linearly, as shown in Fig. 6 (details in Table S1†). For the shortest separation, the antiferromagnetic contribution dominates, but the balance seems to be very subtle, with a very steep transition towards dominant ferromagnetic interactions for only slightly larger separations. The interaction rapidly reaches a maximum of around 4.19 Å, and then decreases smoothly with increasing Gd···Gd distances. Interestingly, the prototype molecular cooler Gd-ac seems to represent the optimal structural configuration for a maximal ferromagnetic exchange. It should be noted that the Gd–O–Gd angle remains in all cases above 112.5°. More acute angles and shorter Gd···Gd separations are likely not accessible with this bridge topology since then additional *syn–syn* carboxylates are favoured. This is clearly shown by comparing with compounds with a B-type bridge (Fig. S8† right).[20,23] All these present Gd–O–Gd angles below 110°, and the corresponding set

of (mostly antiferromagnetic) interaction constants also correlates reasonably, in this case linearly, with the Gd···Gd separation (Fig. S8† left). It is interesting to note that the approximate critical value of the Gd···Gd distance for which the coupling changes the sign is similar for both groups of compounds, at *ca.* 4.12 Å. As originally postulated by Perec *et al.*,[21] these separate correlations found for two types of carboxylate-bridged Gd(III) pairs seem to indicate that more acute Gd–O–Gd and shorter Gd···Gd distance favour the antiferromagnetic contribution to the exchange coupling, through a likely increase of orbital overlap either through the oxygen bridge and/or through space. While these correlations could be used to optimize the MCE of Gd(III)-carboxylate compounds (see Fig. S7† and the aforementioned discussion on the sign of the interaction), it is however obviously difficult to control synthetically the Gd···Gd separation or even the type of bridge formed by carboxylate ligands.

Conclusions

Aiming to modify $[Gd_2(CH_3CO_2)_6(H_2O)_4]\cdot 4H_2O$, the prototype of a truly molecular cooler with ferromagnetic interactions, in order to either suppress its magnetic order or provide it with chemical functions useful for covalent grafting onto surfaces, the infinite coordination chain compounds $[Gd(CH_3CO_2)_3(dmf)]_\infty$ (**1**) and $\{[Gd(HO(CH_2)_3CO_2)_3(H_2O)]\cdot H_2O\}_\infty$ (**2**) have been synthesized. Replacement of coordinated water molecules by dimethylformamide in **1** does impede the presence of a magnetic order due to the absence of intermolecular interactions, but modification of the acetate bridging mode results in switching the magnetic interaction to antiferromagnetic. Replacing acetate ligands by hydroxybutanoate in **2** does succeed in providing a ferromagnetically coupled system with appended hydroxybutyl groups. Magneto-thermal studies indicate a large magneto-caloric effect for both compounds, chiefly ascribed to their large magnetic/non-magnetic element ratios. However, in spite of the relatively larger magnetic density, compound **1** shows a smaller MCE at low applied fields, owing to the negative sign of the exchange interaction. The magnetic interactions at work in both compounds have been discussed in light of magneto-structural correlations, which indicate that the original $[Gd_2(CH_3CO_2)_6(H_2O)_4]\cdot 4H_2O$ material possesses optimal structural parameters, at least among carboxylato-bridged systems. We will now aim to use **2** and similar systems to functionalize surfaces and thus advance towards true on-chip cooling with efficient cryogenic molecular coolers.

Acknowledgements

This work has been supported by the Spanish MINECO and FEDER through grants MAT2011-24284 and MAT2012-38318-C03-01 and by an EU Marie Curie IEF (PIEF-GA-2011-299356 to G. L.). The Advanced Light Source is supported by the Director, Office of Science, Office of Basic Energy Sciences of the U.S. Department of Energy under contract no. DE-AC02-05CH11231.

Notes and references

1 (*a*) M. Evangelisti and E. K. Brechin, *Dalton Trans.*, 2010, **39**, 4672–4676; (*b*) R. Sessoli, *Angew. Chem., Int. Ed.*, 2012, **51**, 43–45; (*c*) J. W. Sharples and D. Collison, *Polyhedron*, 2013, **54**, 91–103.

2 (*a*) A. M. Tishin and Y. I. Spichkin, *The Magnetocaloric Effect and its Applications*, Taylor & Francis, London, 2003; (*b*) M. Evangelisti, Molecule-based magnetic coolers: measurement, design and application, in *Molecular Magnets. Physics and Applications*, ed. F. Luis, J. Bartolomé and J. F. Fernandez, Springer-Verlag, Berlin, Heidelberg, 2014, pp. 365–387.

3 (*a*) B. Daudin, R. Lagnier and B. Salce, *J. Magn. Magn. Mater.*, 1982, **27**, 315–322; (*b*) T. Numazawa, K. Kamiya, T. Okano and K. Matsumoto, *Physica B*, 2003, **329–333**, 1656–1657.

4 High nuclearity $[Gd_x]$ complexes: (*a*) J. W. Sharples, Y. Z. Zheng, F. Tuna, E. J. L. McInnes and D. Collison, *Chem. Commun.*, 2011, **47**, 7650–7652; (*b*) R. J. Blagg, F. Tuna, E. J. L. McInnes and R. E. P. Winpenny, *Chem. Commun.*, 2011, **47**, 10587–10589; (*c*) S.-J. Liu, J.-P. Zhao, J. Tao, J.-M. Jia, S.-D. Han, Y. Li, Y.-C. Chen and X.-H. Bu, *Inorg. Chem.*, 2013, **52**, 9163–9165; (*d*) L.-X. Chang, G. Xiong, L. Wang, P. Cheng and B. Zhao, *Chem. Commun.*, 2013, **49**, 1055–1057; (*e*) F.-S. Guo, Y.-C. Chen, L.-L. Mao, W.-Q. Lin, J.-D. Leng, R. Tarasenko, M. Orendác, J. Prokleska, V. Sechovsky and M.-L. Tong, *Chem. – Eur. J.*, 2013, **19**, 14876–14885.

5 High nuclearity 3d-Gd complexes: (*a*) With Mn see: Y.-Z. Zheng, E. M. Pineda, M. Heliwell and R. E. P. Winpenny, *Chem. – Eur. J.*, 2012, **18**, 4161–4165; (*b*) With Cu see: S. Langley, N. F. Chilton, B. Moubaraki, T. N. Hooper, E. K. Brechin, M. Evangelisti and K. S. Murray, *Chem. Sci.*, 2011, **2**, 1166–1169; (*c*) With Co see: Y.-Z. Zheng, M. Evangelisti, F. Tuna and R. E. P. Winpenny, *J. Am. Chem. Soc.*, 2012, **134**, 1057–1065; (*d*) With Cr see: T. Birk, K. S. Pedersen, C. A. Thuesen, T. Weyhermüller, M. Schau-Magnussen, S. Piligkos, H. Weihe, S. Mossin, M. Evangelisti and J. Bendix, *Inorg. Chem.*, 2012, **51**, 5435–5443; (*e*) With Ni see: Y.-Z. Zheng, M. Evangelisti and R. E. P. Winpenny, *Angew. Chem., Int. Ed.*, 2011, **50**, 3692–3695.

6 3d complexes: (*a*) R. Shaw, R. H. Laye, L. F. Jones, D. M. Low, C. Talbot-Eeckelaers, Q. Wei, C. J. Milios, S. Teat, M. Helliwell, J. Raftery, M. Evangelisti, M. Affronte, D. Collison, E. K. Brechin and E. J. L. McInnes, *Inorg. Chem.*, 2007, **46**, 4968–4978; (*b*) M. Manoli, A. Collins, S. Parsons, A. Candini, M. Evangelisti and E. K. Brechin, *J. Am. Chem. Soc.*, 2008, **130**, 11129–11139.

7 M. Evangelisti, O. Roubeau, E. Palacios, A. Camón, T. N. Hooper, E. K. Brechin and J. J. Alonso, *Angew. Chem., Int. Ed.*, 2011, **50**, 6606–6609.
8 E. Colacio, J. Ruiz, G. Lorusso, E. K. Brechin and M. Evangelisti, *Chem. Commun.*, 2013, **49**, 3845–3847.
9 (*a*) L. Sedláková, J. Hanko, A. Orendácová, M. Orendác, C.-L. Zhou, W.-H. Zhu, B.-W. Wang, Z.-M. Wang and S. Gao, *J. Alloys Compd.*, 2009, **487**, 425–429; (*b*) R. Sibille, T. Mazet, B. Malaman and M. François, *Chem. – Eur. J.*, 2012, **18**, 12970–12973; (*c*) F.-S. Guo, Y.-C. Chen, J.-L. Liu, J.-D. Leng, Z.-S. Meng, P. Vrábel, M. Orendác and M.-L. Tong, *Chem. Commun.*, 2012, **48**, 12219–12221; (*d*) Y.-C. Chen, F.-S. Guo, Y.-Z. Zheng, J.-L. Liu, J.-D. Leng, R. Tarasenko, M. Orendác, J. Proleska, V. Sechovsky and M.-L. Tong, *Chem. – Eur. J.*, 2013, **19**, 13504–13510.
10 G. Lorusso, M. Palacios, G. S. Nichol, E. K. Brechin, O. Roubeau and M. Evangelisti, *Chem. Commun.*, 2012, **48**, 7592–7594.
11 G. Lorusso, J. W. Sharples, E. Palacios, O. Roubeau, E. K. Brechin, R. Sessoli, A. Rossin, E. K. Brechin, F. Tuna, E. J. L. McInnes, D. Collison and M. Evangelisti, *Adv. Mater.*, 2013, **25**, 4653–4656.
12 G. Lorusso, M. Jenkins, P. González-Monje, A. Arauzo, J. Sesé, D. Ruiz-Molina, O. Roubeau and M. Evangelisti, *Adv. Mater.*, 2013, **25**, 2984–2988.
13 *SAINT, SADABS and SHELXTL*, Bruker AXS Inc., Madison, Wisconsin, USA.
14 G. M. Sheldrick, *Acta Crystallogr., Sect. A: Fundam. Crystallogr.*, 2008, **64**, 112–122.
15 F.-S. Guo, J.-D. Leng, J.-L. Liu, Z.-S. Meng and M.-L. Tong, *Inorg. Chem.*, 2012, **51**, 405–413.
16 CSD version 5.33; November 2011 + 4 updates (August 2012).
17 L. Cañadillas-Delgado, O. Fabelo, J. Pasán, F. S. Delgado, F. Lloret, M. Julve and C. Ruiz-Pérez, *Dalton Trans.*, 2010, **39**, 7286–7293.
18 M. E. Fisher, *Am. J. Physiol.*, 1964, **32**, 343–346.
19 The least-squares fit for compound **1** provides a χ^2 of 0.009, while for **2** the best fit gives a χ^2 of 0.06.
20 L. Cañadillas-Delgado, J. Pasán, O. Fabelo, M. Julve, F. Lloret and C. Ruiz-Perez, *Polyhedron*, 2013, **52**, 321–332.
21 R. Baggio, R. Calvo, M. T. Garland, O. Peña, M. Perec and A. Rizzi, *Inorg. Chem.*, 2005, **44**, 8979–8987.
22 (*a*) S. T. Hatscher and W. Urland, *Angew. Chem., Int. Ed.*, 2003, **42**, 2862–2864; (*b*) M. C. Favas, D. L. Kepert, B. W. Skelton and A. H. White, *J. Chem. Soc., Dalton Trans.*, 1980, 454–458; (*c*) A. Rohde and W. Urland, *J. Alloys Compd.*, 2006, **408–412**, 618–621; (*d*) M. Hernández-Molina, C. Ruiz-Pérez, T. López, F. Lloret and M. Julve, *Inorg. Chem.*, 2003, **42**, 5456–5458; (*e*) A. Rohde and W. Urland, *Z. Anorg. Allg. Chem.*, 2005, **631**, 417–420; (*f*) L. Cañadillas-Delgado, O. Fabelo, J. Cano, J. Pasán, F. S. Delgado, F. Lloret, M. Julve and C. Ruiz-Pérez, *CrystEngComm*, 2009, **11**, 2131–2142; (*g*) N. Xu, W. Shi, D.-Z. Liao, S.-P. Yan and P. Cheng, *Inorg. Chem.*, 2008, **47**, 8748–8756.
23 (*a*) J.-P. Costes, J. M. Clemente-Juan, F. Dahan, F. Nicodème and M. Verelst, *Angew. Chem., Int. Ed.*, 2002, **41**, 323–325; (*b*) D. John and W. Urland, *Eur. J. Inorg. Chem.*, 2006, 3503–3509; (*c*) D. John and W. Urland, *Z. Anorg. Allg. Chem.*, 2005, **631**, 2635–2637; (*d*) D. John and W. Urland, *Eur. J. Inorg. Chem.*, 2005, 4486–4489; (*e*) A. Panagiotopoulos, T. F. Zafiropoulos, S. P. Perlepes, E. Bakalbassis, I. Masson-Ramade, O. Kahn, A. Terzis and C. P. Raptopoulou, *Inorg. Chem.*, 1995, **34**, 4918–4920; (*f*) A. W.-H. Lam, W.-T. Wong, S. Gao, G. Wen and X.-X. Zhang, *Eur. J. Inorg. Chem.*, 2003, 149–163.